Applied Physics Letters

Contact resistance at graphene/MoS_2 lateral heterostructures

Cite as: Appl. Phys. Lett. **114**, 163101 (2019); https://doi.org/10.1063/1.5083133
Submitted: 28 November 2018 . Accepted: 11 April 2019 . Published Online: 23 April 2019

M. Houssa, K. Iordanidou, A. Dabral, A. Lu, R. Meng, G. Pourtois, V. V. Afanas'ev, and A. Stesmans

ARTICLES YOU MAY BE INTERESTED IN

Rapid-throughput solution-based production of wafer-scale 2D MoS_2
Applied Physics Letters **114**, 163102 (2019); https://doi.org/10.1063/1.5093039

Electron redistribution and energy transfer in graphene/MoS_2 heterostructure
Applied Physics Letters **114**, 113103 (2019); https://doi.org/10.1063/1.5088512

Two-dimensional charge carrier distribution in MoS_2 monolayer and multilayers
Applied Physics Letters **114**, 101602 (2019); https://doi.org/10.1063/1.5078711

© 2019 Author(s).

Applied Physics Letters ARTICLE scitation.org/journal/apl

Contact resistance at graphene/MoS_2 lateral heterostructures

Cite as: Appl. Phys. Lett. **114**, 163101 (2019); doi: 10.1063/1.5083133
Submitted: 28 November 2018 · Accepted: 11 April 2019 ·
Published Online: 23 April 2019

M. Houssa,[1,a)] K. Iordanidou,[2] A. Dabral,[1,3] A. Lu,[4] R. Meng,[1] G. Pourtois,[3] V. V. Afanas'ev,[1] and A. Stesmans[1]

AFFILIATIONS

[1]Department of Physics and Astronomy, University of Leuven, B-3001 Leuven, Belgium
[2]Department of Physics, University of Oslo, NO-0316 Oslo, Norway
[3]imec, Kapeldreef 75, B-3001 Leuven, Belgium
[4]MathAM-OIL, AIST, Sendai 980-8577, Japan

[a)]Author to whom correspondence should be addressed: michel.houssa@kuleuven.be.

ABSTRACT

The contact resistance at two-dimensional graphene/MoS_2 lateral heterojunctions is theoretically studied, using first-principles simulations based on density functional theory and the nonequilibrium Green's function method. The computed contact resistance lies in the range of 10^2 to 10^4 Ω μm, depending on the contact edge symmetry (armchair or zigzag) and termination (Mo and/or S terminated). This large variation in the contact resistance arises from the variation in the interface barrier height, which is sensitive to the presence of polar C-Mo bonds or sulfur dangling bonds at the interface. These results highlight that the control of the edge symmetry and/or edge termination is crucial to achieve a low contact resistance (in the range of a few hundred ohms micrometer) at graphene/MoS_2 lateral heterojunctions for 2D material-based field-effect devices.

Published under license by AIP Publishing. https://doi.org/10.1063/1.5083133

Two-dimensional (2D) materials like graphene and transition metal dichalcogenides are currently triggering a lot of interest, due to their potential applications in future nanoelectronic devices.[1–5] These materials indeed offer the possibility to scale the channel thickness of field-effect transistors down to the atomic level, leading to an optimized electrostatic control of the charge carriers in these devices. The formation of 2D heterostructures, either by the van der Waals stacking of different 2D materials or via the formation of 2D lateral heterojunctions, also paves the way for the fabrication of devices with unique electronic, optoelectronic, or magnetic properties.[6–11]

The contact resistance R_c is a critical issue in these 2D material-based devices. Contact resistances at bulk metal/2D semiconductor interfaces are typically in the range of 10^3–10^5 Ω μm,[12] limiting the device performances. Although bulk metal/2D semiconductor edge contacts enable us to reduce the contact resistance (as compared to top contacts),[12,13] R_c still lies in the range of kilohms micrometer, being typically an order of magnitude too large for field-effect transistor applications. On the other hand, lateral graphene/MoS_2 interfaces have been fabricated recently and studied theoretically.[14–18] These interfaces provide a promising platform for realizing low contact resistance between a 2D metal (graphene) and a 2D semiconductor (like MoS_2) and are thus of potential interest for 2D material-based devices.

In this work, we have theoretically studied the contact resistance R_c of graphene/MoS_2 lateral heterostructures, using density functional theory (DFT) and the nonequilibrium Green's function method (NEGF). Different interface models have been considered based on the edge contact symmetry (armchair or zigzag) and edge termination (Mo and/or S). The contact resistance is found to be strongly dependent on the edge symmetry/termination, which can be correlated with the absence or the presence of polar bonds (C-Mo) or defects (sulfur dangling bonds) at the interface.

Four graphene/MoS_2 lateral heterostructures are considered, with different contact edge symmetries and/or terminations, as shown in Fig. 1. Large supercells are employed, containing typically about 250 atoms, in order to minimize the strain in the graphene and MoS_2 layers, due to their different computed lattice constants (2.47 Å for graphene and 3.17 Å for MoS_2); the residual strain in both layers is typically about 1.5% (compressive in graphene and tensile in MoS_2). The atomic relaxation and electronic structure calculations of the graphene/MoS_2 interface models are performed using DFT as implemented in the Siesta package.[19] The generalized gradient approximation (GGA) is used for the exchange-correlation functional.[20] Core electrons are described by norm-conserving pseudopotentials,[21] and valence electrons are described using double-zeta

Published under license by AIP Publishing

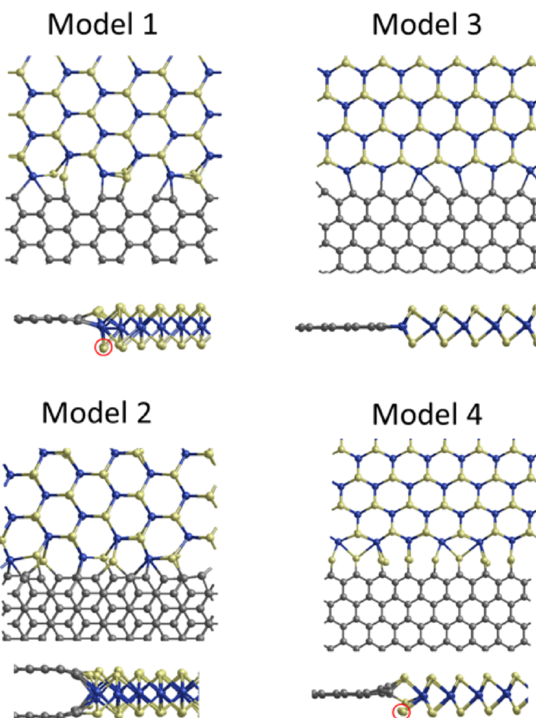

FIG. 1. Top and side views of the relaxed atomic configurations of lateral graphene/MoS_2 interface models. Model 1 and model 2 correspond to armchair edge contacts, with a single graphene layer and a double graphene layer, respectively. Models 3 and 4 correspond to zigzag edge contacts with Mo termination and S termination, respectively. Dark gray, blue, and yellow spheres correspond to C, Mo, and S atoms, respectively. The S dangling bonds in model 1 and model 4 are encircled in red.

polarized basis sets. The energy cut-off is fixed to 300 Ry, and a $(2\times2\times1)$ and $(15\times15\times1)$ Monkhorst-Pack k-point mesh is used for the structural relaxations and electronic structure calculations, respectively. The convergence threshold for the residual atomic forces is fixed to 0.01 eV/Å. The calculations are performed by including self-consistent dipole corrections, which are particularly important for computing the energies and work functions of slab models including a net dipole moment.[22]

The ballistic transport simulations are performed using the non-equilibrium Green's function method, as implemented in the TranSiesta package.[23] Single-zeta polarized basis sets are used for the transport simulations. The system is separated into three different parts along the transport direction, namely, the left electrode (graphene), the central channel region (MoS_2), and the right electrode (graphene). For each considered graphene/MoS_2 heterostructure, the graphene contact lengths and contact widths are about 1 nm and 2 nm, respectively, and the MoS_2 channel length is about 2.5 nm. The conductance G is computed using the Landauer equation[24]

$$G=\frac{2e^2}{h}\int T(E,V)\left(\frac{-\partial f^0}{\partial E}\right)dE, \tag{1}$$

where T(E, V) is the transmission probability, which is computed using the equation

$$T(E,V)=Trace\left[\Gamma_L G^R \Gamma_R G^A\right], \tag{2}$$

where G^R and G^A are the retarded and advanced Green's functions and $\Gamma_{L/R}$ are the self-energies of the left and right contacts, which include the energy dissipation at these contacts. For the complex contour integration, ten points on the line part and thirty points along the arc part are used. The contact resistance $R_c = 1/G$ is computed from Eqs. (1) and (2) at a fixed bias of 0.5 V, assuming that energy dissipation arises solely from the contacts; the MoS_2 channel is indeed defect free, and carrier transport is expected to be purely ballistic along the channel.

The four relaxed graphene/MoS_2 interface models are shown in Fig. 1. Model 1 is based on an armchair-edge contact with a single graphene layer. Both C-Mo and C-S bonds are formed at the interface with average bond lengths of 2.14 Å and 1.83 Å, respectively. Sulfur dangling bonds (from the bottom sulfur sublayer) are also present at this interface. In model 2, a graphene bilayer is used, which enables us to saturate all the S dangling bonds of the armchair edge MoS_2 layer, by forming C-S bonds. Model 3 is based on a zigzag-edge contact, terminated by Mo atoms. After relaxation, only C-Mo bonds (with an average bond length of 2.13 Å) are formed, and the interface is "defect free." Model 4 is based on a S-terminated zigzag edge contact. In this case, only C-S bonds (with an average bond length of 1.79 Å) are formed, but sulfur dangling bonds are still present in the bottom S sublayer.

The interface formation energy γ of the graphene/MoS_2/graphene heterostructures is computed using the expression[25,26]

$$\gamma=\frac{1}{2L}\left(E_{total}-n_C\mu_C-n_{MO}\mu_{MoS_2}-\Delta n_S\mu_S\right), \tag{3}$$

where L is the interface length (the factor 2 accounts for the presence of two graphene/MoS_2 interfaces for symmetric slabs), E_{total} is the total energy of the graphene/MoS_2/graphene slab, and n_i and μ_i correspond to the number of atoms and their chemical potentials, respectively, μ_{MoS2} is the total energy of a MoS_2 (monolayer) unit cell, and $\Delta n_S = n_S - 2n_{Mo}$. The chemical potential μ_{Mo} was fixed to the one corresponding to body-centered cubic Mo and $\mu_S = ½ (\mu_{MoS2} - \mu_{Mo})$ in the Mo-rich limit and $\mu_S = \mu_{S(bulk)}$ in the S-rich limit, where $\mu_{S(bulk)}$ corresponds to the chemical potential of sulfur in an S_8 ring.[26]

The interface formation energy γ is given in Table I for the different interface models shown in Fig. 1. In the Mo-rich limit, the Mo-terminated zigzag interface model (model 3) is predicted to be the most stable one. In the S-rich limit, the armchair interface model, with a bilayer graphene layer, gives the lowest interface formation energy. Considering the zigzag-edge interface models, the Mo and S edge-terminations have comparable interface energies (within 0.1 eV/Å),

TABLE I. Computed interface formation energies γ of the different graphene/MoS_2 interface models shown in Fig. 1, in the Mo-rich and S-rich limit. The value of the computed contact resistance R_c of each interface model is also given.

	γ (eV/Å) Mo-rich limit	γ (eV/Å) S-rich limit	R_c (Ω μm)
Model 1	2.4	2.4	8.1×10^3
Model 2	1.5	1.5	5.6×10^2
Model 3	1.2	1.8	2.2×10^2
Model 4	2.6	1.9	2.3×10^4

Published under license by AIP Publishing

indicating that both interfaces could be produced during a S-rich growth process.

The computed contact resistance R_c of the different interface models is also indicated in Table I. The contact resistances for the defect-free interface models (models 2 and 3) typically lie between 220 and 560 Ω μm, being close to the target values for nanoscale field-effect transistors.[12] In contrast, the contact resistance is about 2 orders of magnitude larger at graphene/MoS_2 interfaces with S dangling bonds. One should note that the graphene/MoS_2 heterostructures investigated here are undoped. Since the contact resistance at 2D materials should decrease with interfacial doping[27] and/or channel doping,[28] further reduction of R_c can be expected at doped graphene/MoS_2 contacts.

To gain insight into these results, the transmission probabilities and electrostatic potential profiles of the Mo and S terminated zigzag interface models (models 3 and 4, respectively) are discussed below. The computed transmission spectra (at zero bias) and the electrostatic potential profile of the Mo-terminated zigzag interface model are shown in Figs. 2(a) and 2(b), respectively. The onset of transmission is at about 0.1 eV from the Fermi level (for the positive energies). This result is consistent with the energy barrier height Φ_B of about 0.1 eV, extracted from the electrostatic potential profile shown in Fig. 2(b), as well as from the contribution of graphene and MoS_2 to the electronic density of states, shown in the inset of Fig. 2(a). The barrier height is close to the difference between the computed graphene work function (4.4 eV) and MoS_2 electron affinity (4.2 eV). The barrier height is reduced by about 0.1 eV from the ideal value (Schottky limit), due to the presence of polar C-Mo bonds, forming a dipole layer at the interface; due to the electronegativity difference between C and Mo, electrons are transferred from Mo atoms to C atoms. These C-Mo bonds significantly contribute to the electronic density of states near the Fermi level, as shown in the isosurface charge density plot in the inset of Fig. 2(a).

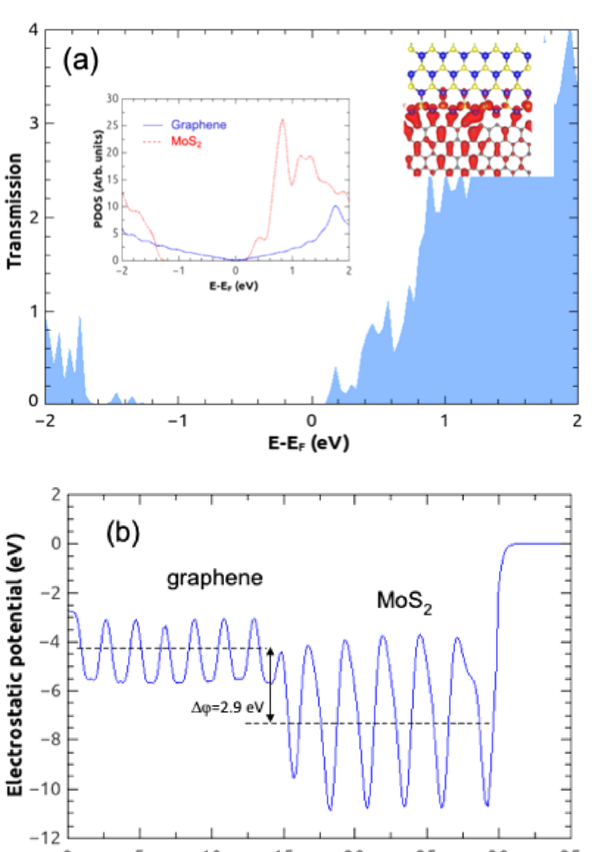

FIG. 2. (a) Computed transmission spectra (at zero bias) of a graphene/MoS_2 lateral heterostructure with Mo-terminated zigzag edge contacts (model 3 in Fig. 1). The Fermi level corresponds to the reference (zero) energy. The insets show the partial density of states (PDOS) of graphene and MoS_2 and the isosurface (0.01 e/Å^3) charge density near the Fermi level. (b) Electrostatic potential along the same graphene/MoS_2 lateral heterostructure. $\Delta\varphi$ corresponds to the difference between the average electrostatic potentials of graphene and MoS_2 (indicated by the dashed lines).

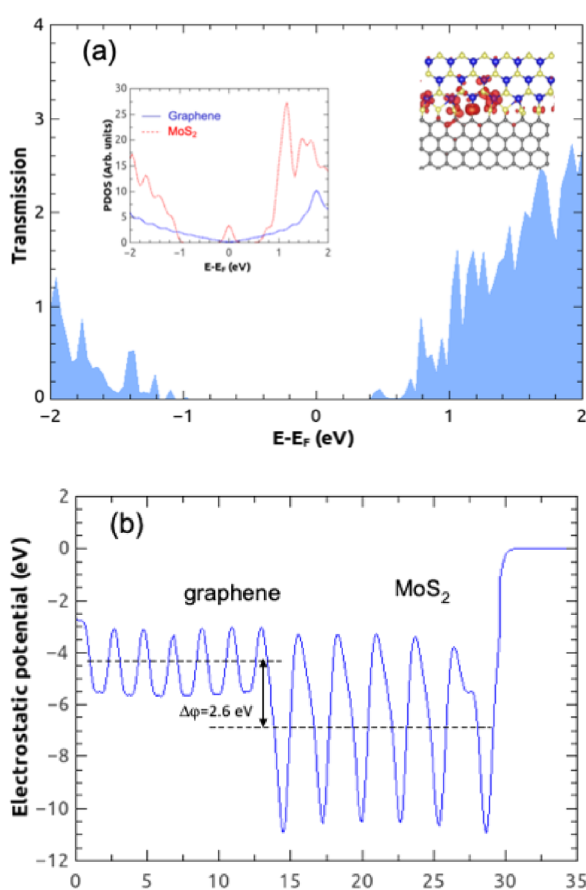

FIG. 3. (a) Computed transmission spectra (at zero bias) of a graphene/MoS_2 lateral heterostructure with S-terminated zigzag edge contacts (model 4 in Fig.1). The Fermi level corresponds to the reference (zero) energy. The insets show the partial density of states (PDOS) of graphene and MoS_2 and the isosurface (0.01 e/Å^3) charge density near the Fermi level. (b) Electrostatic potential along the same graphene/MoS_2 lateral heterostructure. $\Delta\varphi$ corresponds to the difference between the average electrostatic potentials of graphene and MoS_2 (indicated by the dashed lines).

Published under license by AIP Publishing

For comparison, the zero-bias transmission probability and the electrostatic potential profile of the S-terminated zigzag interface model, with a large density of S dangling bonds (model 4) are shown in Figs. 3(a) and 3(b), respectively. In this case, the onset of the transmission probability is at about 0.4 eV from the Fermi level. The transmission is significantly reduced, compared to the Mo-terminated interface. An upward shift of the offset $\Delta\varphi$ between the average electrostatic potential of graphene and MoS_2 of about 0.3 eV (as compared to the Mo-terminated interface) is also observed in Fig. 3(b), corresponding to an increase in Φ_B of about 0.3 eV.[29] In this case, the S dangling bonds introduce gap states at about 0.4–0.5 eV below the MoS_2 conduction band, and the Fermi level is pinned by these states, as evidenced from the partial electronic density of states, shown in the inset of Fig. 3(a); the isosurface charge density plot, also shown in the inset of Fig. 3(a), indeed indicates that the S dangling bonds contribute significantly to the electronic density of states near the Fermi level. During the formation of the graphene/MoS_2 junction, the S dangling bonds are negatively charged and the barrier height is determined by the charge neutrality level of these defects, leading to an interface barrier Φ_B of about 0.4 eV.

The contact resistance of the different interface models is shown in Fig. 4, as a function of the barrier height Φ_B. A clear correlation between R_c and Φ_B is revealed, with low R_c values being calculated for defect-free interfaces. The pinning of the Fermi level by the S dangling bonds results in a larger barrier for interface models 1 and 4, increasing the contact resistance by about two orders of magnitude.

In summary, the contact resistance of several graphene/MoS_2 lateral heterostructures has been computed from first-principles simulations. Defect-free interfaces, as obtained from armchair edge bilayer graphene/MoS_2 or Mo-terminated zigzag edge single layer graphene/MoS_2 heterojunctions, are predicted to have low contact resistances, in the range of a few hundred ohms micrometer. Such contact resistances are very promising for 2D material-based field-effect devices. However, defects like S dangling bonds, present at armchair single layer graphene/MoS_2 contacts or S terminated zigzag edge contacts, have a detrimental impact on the contact resistance, which is increased by about two orders of magnitude at these interfaces. Achieving a low contact resistance at graphene/MoS_2 later heterojunctions will thus critically depend on the control of the edge symmetry and/or edge termination.

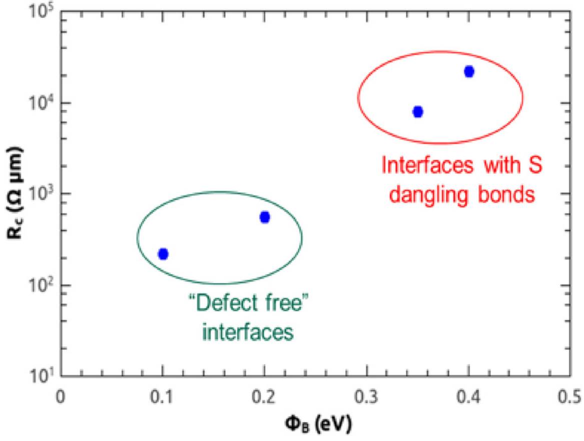

FIG. 4. Contact resistance as a function of the calculated barrier height Φ_B in the different graphene/MoS_2 interface models, on a semilog scale.

Part of this work was financially supported by the KU Leuven Research Funds, Project No. C14/17/080, as well as the 2DFun project, an ERA-NET project in the framework of the Graphene Flagship. The authors acknowledge the support from Flanders Innovation and Entrepreneurship.

REFERENCES

[1] S. Z. Butler, S. M. Hollen, L. Y. Cao, Y. Cui, J. A. Gupta, H. R. Gutiérrez, T. F. Heinz, S. S. Hong, J. X. Huang, A. F. Ismach *et al.*, "Progress, challenges, and opportunities in two-dimensional materials beyond graphene," ACS Nano **7**, 2898 (2013).
[2] G. Fiori, F. Bonaccorso, G. Iannaccone, T. Palacios, D. Neumaier, A. Seabaugh, S. K. Banerjee, and L. Colombo, "Electronics based on two-dimensional materials," Nat. Nanotechnol. **9**, 768 (2014).
[3] F. Schwierz, J. Pezoldt, and R. Granzner, "Two-dimensional materials and their prospects in transistor electronics," Nanoscale **7**, 8261 (2015).
[4] A. Molle, J. Goldberger, M. Houssa, Y. Xu, S. C. Zhang, and D. Akinwande, "Buckled two-dimensional Xene sheets," Nat. Mater. **16**, 163 (2017).
[5] J. A. Robinson, "2D for beyond CMOS," APL Mater. **6**, 058202 (2018).
[6] A. K. Geim and I. V. Grigorieva, "Van der Waals heterostructures," Nature **499**, 419 (2013).
[7] C. Huang, S. Wu, A. M. Sanchez, J. J. P. Peters, R. Beanland, J. S. Ross, P. Rivera, W. Yao, D. H. Cobden, and X. Xu, "Lateral heterojunctions with monolayer $MoSe_2$-WSe_2 semiconductors," Nat. Mater. **13**, 1096 (2014).
[8] Y. Gong, J. Lin, X. Wang, G. Shi, S. Lei, Z. Lin, X. Zou, G. Ye, R. Vajtai, B. I. Yakobson, H. Terrones, M. Terrones, B. K. Tay, J. Lou, S. T. Pantelides, Z. Liu, W. Zhou, and P. M. Ajayan, "Vertical and in-plane heterostructures from WS_2/MoS_2 monolayers," Nat. Mater. **13**, 1135 (2014).
[9] Q. A. Vu, J. H. Lee, V. L. Nguyen, Y. S. Shin, S. C. Lim, K. Lee, J. Heo, S. Park, K. Kim, and Y. H. Lee, "Tuning carrier tunneling in van der Waals heterostructures for ultrahigh detectivity," Nano Lett. **17**, 453 (2017).
[10] C. Zhang, M. Y. Li, J. Tersoff, Y. Han, Y. Su, L. J. Li, D. A. Muller, and C. K. Shih, "Strain distributions and their influence in electronic structures of WSe_2-MoS_2 laterally strained heterojunctions," Nat. Nanotechnol. **13**, 152 (2018).
[11] D. Unuchek, A. Ciarrocchi, A. Avsar, K. Watanabe, T. Taniguchi, and A. Kis, "Room-temperature electrical control of exciton flux in a van der Waals heterostructure," Nature **560**, 340 (2018).
[12] A. Allain, J. Kang, K. Banerjee, and A. Kis, "Electrical contacts to two-dimensional semiconductors," Nat. Mater. **14**, 1195 (2015).
[13] G. Yoo, S. Lee, B. Yoo, C. Han, S. Kim, and M. S. Oh, "Electrical contact analysis of multilayer MoS_2 transistor with molybdenum source/drain electrodes," IEEE Electron Device Lett. **36**, 1215 (2015).
[14] J. Meng, H. D. Song, C. Z. Li, Y. Jin, L. Tang, D. Liu, Z. M. Liao, F. Xiu, and D. P. Yu, "Lateral graphene p-n junctions formed by the graphene/MoS_2 hybrid interface," Nanoscale **7**, 11611 (2015).
[15] M. H. D. Guimaraes, H. Gao, Y. Han, K. Kang, S. Xie, C. J. Kim, D. A. Muller, D. C. Ralph, and J. Park, "Atomically thin ohmic edge contacts between two-dimensional materials," ACS Nano **10**, 6392 (2016).
[16] M. Zhao, Y. Ye, Y. Han, Y. Xia, H. Zhu, S. Wang, Y. Wang, D. A. Muller, and X. Zhang, "Large-scale chemical assembly of atomically thin transistors and circuits," Nat. Nanotechnol. **11**, 954 (2016).
[17] X. Ling, Y. Lin, Q. Ma, Z. Wang, Y. Song, L. Yu, S. Huang, W. Fang, X. Zhang, A. L. Hsu, Y. Bie, Y.-H. Lee, Y. Zhu, L. Wu, J. Li, P. Jarillo-Herrero, M. Dresselhaus, T. Palacios, and J. Kong, "Parallel stitching of 2D materials," Adv. Mater. **28**, 2322 (2016).
[18] X. Liu, J. Gao, G. Zhang, and Y. W. Zhang, "MoS_2-graphene in-plane contact for high interfacial thermal conduction," Nano Res. **10**, 2944 (2017).
[19] J. M. Soler, E. Artacho, J. D. Gale, A. Garcia, J. Junquera, P. Ordejon, and D. Sanchez-Portal, "The Siesta method for ab initio order-N materials simulations," J. Phys.: Condens. Matter **14**, 2745 (2002).

Published under license by AIP Publishing

[20]J. P. Perdew, K. Burke, and M. Ernzerhof, "Generalized gradient approximation made simple," Phys. Rev. Lett. **77**, 3865 (1996).
[21]N. Trouiller and J. L. Martins, "Efficient pseudopotentials for plane-wave calculations," Phys. Rev. B **43**, 1993 (1991).
[22]L. Bengtsson, "Dipole correction for surface supercell calculations," Phys. Rev. B **59**, 12301 (1999).
[23]M. Brandbyge, J. L. Mozos, P. Ordejon, J. Taylor, and K. Stokbro, "Density-functional method for nonequilibrium electron transport," Phys. Rev. B **65**, 165401 (2002).
[24]S. Datta, *Electronic Transport in Mesoscopic Systems* (Cambridge University Press, Cambridge, UK, 1995).
[25]M. V. Bollinger, K. W. Jacobsen, and J. K. Nørskov, "Atomic and electronic structure of MoS_2 nanoparticles," Phys. Rev. B **67**, 085410 (2003).
[26]W. Chen, Y. Yang, Z. Zhang, and E. Kaxiras, "Properties of in-plane graphene/MoS_2 heterojunctions," 2D Mater. **4**, 045001 (2017).
[27]L. Wang, I. Meric, P. Y. Huang, Q. Gao, Y. Gao, H. Tran, T. Taniguchi, K. Watanabe, L. M. Campos, and D. A. Muller, "One-dimensional electrical contact to a two-dimensional material," Science **342**, 614 (2013).
[28]D. Jena, K. Banerjee, and G. H. Xing, "2D crystal semiconductors intimate contacts," Nat. Mater. **13**, 1076 (2014).
[29]R. T. Tung, "The physics and chemistry of the Schottky barrier height," Appl. Phys. Rev. **1**, 011304 (2014).

Published under license by AIP Publishing